A novel design for single-polarization single-mode photonic crystal fiber at 1550 nm

Fangdi Zhang (张方迪), Xiaoyi Liu (刘小毅), Min Zhang (张 民), and Peida Ye (叶培大)

Key Laboratory of Optical Communication and Lightwave Technology, Ministry of Education, Beijing University of Posts and Telecommunications, Beijing 100876

Received October 25, 2006

The present paper proposes a novel design for achieving single-polarization single-mode (SPSM) operation at 1550 nm in photonic crystal fiber (PCF), using a rectangular-lattice PCF with two lines of three central air holes enlarged. The proposed PCF composed entirely of silica material is modeled by a full-vector finite element method with anisotropic perfectly matched layers. Simulations show that single-polarization operation within broad wavelength range can be easily realized with the proposed structure. The wide-band SPSM operation features, the low confinement losses, and the small effective mode area are the main advantages of the proposed PCF structure. A SPSM-PCF with confinement loss less than 0.1 dB/km within wavelength range from 1370 to 1610 nm and effective mode area about 4.7 μm^2 at 1550 nm is numerically demonstrated.

OCIS codes: 060.2280, 060.2310, 060.2420, 060.2430.

Photonic crystal fibers (PCFs) consisting of a core surrounded by a cladding region with multiple air holes were first proposed by Knight *et al.*[1]. Light in PCFs is strongly confined in the transverse plane and can propagate along only the longitudinal direction in the core region. According to the difference in light-guiding mechanism, PCFs can be divided into two different types. The first experimental reported-type guides light by total internal reflection (TIR) between the core and the cladding region with multiple air holes, and such fibers are known as index-guiding PCFs[1,2]. In the second type of fibers, guidance is provided by photonic band gap (PBG) effect exhibited by a perfect periodic structure in the cladding region, allowing for many interesting features such as light confinement to a low-index core[3].

Many unique properties such as wide single-mode wavelength range and anomalous group velocity dispersion are found in this newly proposed fiber[4−8]. By having different air-hole diameters along the two orthogonal axes, PCFs with high modal birefringence can be easily achieved, because the index contrast is higher than that in conventional fibers[9]. Untill now, various types of highly birefringent PCFs have been proposed[9−13]. These fibers have been demonstrated to have a modal birefringence in the order of 10^{-3}, which is almost 10 times of that of the conventional birefringent fibers. Early research has shown that fibers can be designed to operate in a single-polarization regime in which only one polarization mode is guided[14−16]. In these fibers single-polarization operation is realized by using a highly elliptical core, a bow tie structure, or by introducing absorbent material along the core. However, it is observed that the single-polarization bandwidth of these fibers was not more than 180 nm, making it difficult to meet the progressive bandwidth requirement. Recently, it has been shown that highly birefringent PCFs have the potential ability to realize wide-band single-polarization fibers[17−21].

In this paper, we demonstrate a novel design for achieving single-polarization single-mode (SPSM) operation at 1550 nm. The proposed PCF is based on a rectangular-lattice PCF with two lines of three central air holes enlarged. The influence of varying PCF parameters on the properties of SPSM operation is discussed and simulations show that single-polarization operation within broad wavelength range can be easily realized with the proposed structure. A SPSM-PCF with confinement loss less than 0.1 dB/km within wavelength range from 1370 to 1610 nm and effective mode area about 4.7 μm^2 at 1550 nm is numerically obtained.

The cross section of the birefringent PCF we propose for achieving single-polarization operation is shown in Fig. 1. It is a rectangular-lattice fiber structure with two lines of central air holes enlarged. Here parameters Λ and Λ_y are hole pitches (the hole-to-hole distance) in the x and y directions, and d and d' are the diameters of the small and large circular air-holes, respectively. The background material is regular silica with refractive index obtained by the three-order Sellmeier equation[22]. For simplicity, parameters Λ_y and d are chosen to be 0.8Λ and 0.50Λ, respectively.

In our simulations, the full-vector finite element method (FEM) with hybrid edge/nodal element based on

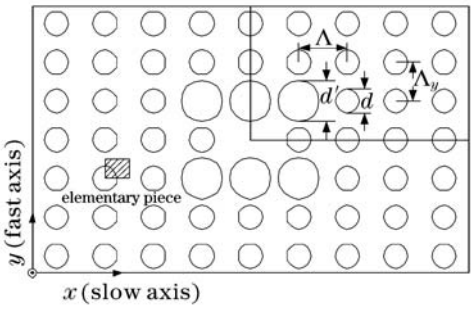

Fig. 1. Cross section of proposed birefringent PCF with six central air holes enlarged. Λ and Λ_y are the hole pitches (hole-to-hole distance) in the x- and y-directions, and d and d' are the diameters of the small and large air holes, respectively.

1671-7694/2007/050260-04

constant tangential and linear normal vector basis functions is applied to analyse the properties of the proposed fiber[20]. In order to evaluate the confinement loss and to eliminate the influence of artificial outer boundaries, anisotropic perfectly matched layers as absorbing boundary condition are applied[20]. After applying the standard finite element procedure, a complex generalized eigenvalue equation is established. Then, the effective index $n_{\rm eff}$ of the mode is determined by

$$n_{\rm eff} = {\rm Re}(\beta/k_0), \tag{1}$$

where k_0 is the free space wave number, and β is the propagation constant obtained by solving the eigenvalue equation. From the imaginary part of β the confinement loss $L_{\rm c}$ for the corresponding mode is derived,

$$L_{\rm c} = 10^3 \cdot \frac{20}{\ln 10} {\rm Im}\beta \ [{\rm dB/km}]. \tag{2}$$

We consider a PCF as shown in Fig. 1 with $\Lambda = 2.2$ μm, $\Lambda_y = 0.8\Lambda$, $d'/\Lambda = 0.85$ and $d/\Lambda = 0.50$. The number of the air-hole rings in the cladding region ($N_{\rm r}$) is assumed to be 10. Figure 2 shows the effective index of the x-polarized mode (solid line) and y-polarized mode (dashed line) as a function of wavelength for the fiber. The effective index of the fundamental space-filling mode (FSM)[2] calculated by applying the FEM to the elementary piece as shown in Fig. 1, is also included in Fig. 2. Due to the symmetric nature of the PCF, only one quarter of the cross section was considered in the simulation. It is interesting to find that two curves, $n_{{\rm FSM}x}$ for x-polarized FSM (chain line) and $n_{{\rm FSM}y}$ for y-polarized FSM (dotted line), respectively exist. This is because the air holes in the cladding region are arranged in rectangular lattice and the FSMs do not degenerate any more. From Fig. 2 we can learn that the effective index of the x polarization mode (slow-axis mode) $n_{\rm s}$ is larger than that of y polarization mode (fast-axis mode) $n_{\rm f}$, and $n_{{\rm FSM}y}$ is higher than $n_{{\rm FSM}x}$. It is acknowledged that when $n_{\rm s}$ is higher than $n_{{\rm FSM}x}$, or $n_{\rm f}$ is higher than $n_{{\rm FSM}y}$, the mode is guided, if not, the mode cuts off. So it is easier to achieve wide-band single-polarization operation in PCF with air holes arranged in rectangular lattice than in hexagonal lattice in Ref. [17], in which the x- and y-polarized FSMs degenerate and the two curves of FSMs become the same one. This is why we choose

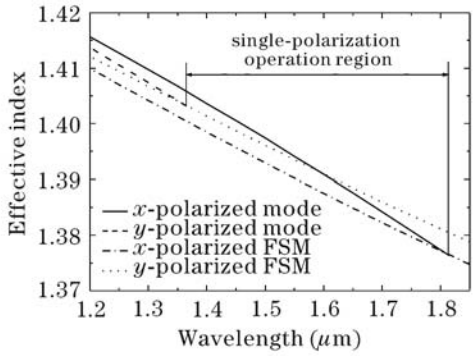

Fig. 2. Effective indices of two orthogonal polarization modes and fundamental space-filling modes for the proposed PCF in Fig. 1 with $\Lambda = 2.2$ μm, $\Lambda_y = 0.8\Lambda$, $d'/\Lambda = 0.85$ and $d/\Lambda = 0.50$.

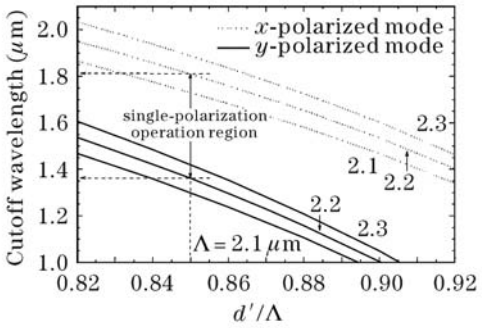

Fig. 3. Cutoff wavelength for the two orthogonal polarization modes as a function of d'/Λ with different Λ.

PCF with air holes arranged in a rectangular lattice structure to study.

For the given combination of parameters, the cutoff wavelengths of y- and x-polarized modes are estimated to be 1370 and 1820 nm, respectively, according to the intersection points of their effective index curves and that of the cladding index as indicated in Fig. 2.

Figure 3 shows the cutoff wavelengths of two orthogonal polarization modes as a function of d'/Λ with $\Lambda_y = 0.8\Lambda$ and $d/\Lambda = 0.50$. Since the effective index is dominated by inner-ring air holes in PCF[23], only five rings of air holes in the cladding region is considered in Fig. 3. Also included in Fig. 3 is the influence of the variation of Λ on the cutoff wavelengths. As seen from Fig. 3, single-polarization operation region shows great dependence on d'/Λ and Λ. Continuous increment of d'/Λ or decrement of Λ down-shifts the single-polarization wavelength region to short wavelengths. The single-polarization operation region of PCF with $\Lambda = 2.2$ μm, $\Lambda_y = 0.8\Lambda$, $d'/\Lambda = 0.85$ and $d/\Lambda = 0.50$, as shown in Fig. 2, are also indicated in Fig. 3.

It has been shown above that wide-band single-polarization operation can be easily achieved in the proposed structure. However, in practical applications only wide-band single-polarization characteristics may not be enough for the usefulness of the fiber. Low confinement losses are also required. In Fig. 4 we show the impact of the number of air-hole rings ($N_{\rm r}$) in the cladding region to the confinement loss obtained by Eq. (2) as a function of wavelength. PCFs in Fig. 1 with $N_{\rm r} = 4$, 6, 8 and 10 are respectively analyzed. We can see from Fig. 4 that

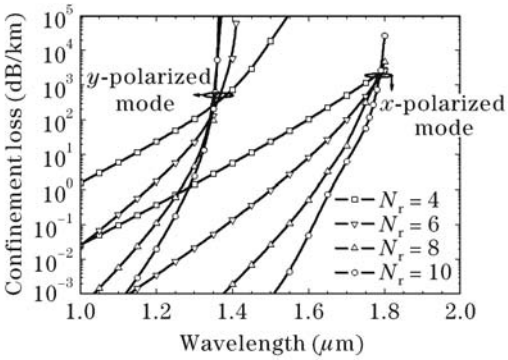

Fig. 4. Confinement loss as a function of wavelength for two orthogonal polarization modes with $\Lambda = 2.2$ μm, $\Lambda_y = 0.8\Lambda$, $d'/\Lambda = 0.85$ and $d/\Lambda = 0.50$, respectively for different $N_{\rm r}$.

confinement loss for guided modes decreases with the increment of N_r, while for unguided modes the reverse is true. It is well known that modes in PCFs with finite number of air holes in the cladding region are inherently leaky[24]. However, this problem for guided modes can be efficiently solved by increasing the number of the air-hole layers. To achieve single-polarization operation within wavelengths longer than 1370 nm and confinement loss less than 0.1 dB/km at 1550 nm, at least 10 rings of air holes are required. As can be seen from Fig. 4, PCF with $\Lambda = 2.2$ μm, $\Lambda_y = 0.8\Lambda$, $d'/\Lambda = 0.85$, $d/\Lambda = 0.50$ and $N_r = 10$ functions as a SPSM one at wavelengths ranging from 1370 to 1610 nm, where only a slow-axis mode is guided and the confinement loss is less than 0.1 dB/km.

We have shown that the proposed fiber possesses many remarkable characteristics such as wide-band single-polarization operation and low confinement loss. Next we will show that our proposed PCF structure has additional characteristics as small effective mode area, which is required for some particular applications such as nonlinear ones. Figure 5 shows the calculated effective mode area of x-polarized mode as a function of wavelength for the optimized parameters $\Lambda = 2.20$ μm, $\Lambda_y = 0.8\Lambda$, $d'/\Lambda = 0.85$, $d/\Lambda = 0.50$, and $N_r = 10$. It also shows the confinement loss. From Fig. 5 we can clearly observe a relatively low effective mode area (4.7 μm^2 at $\lambda = 1550$ nm). From the total intensity distribution of the

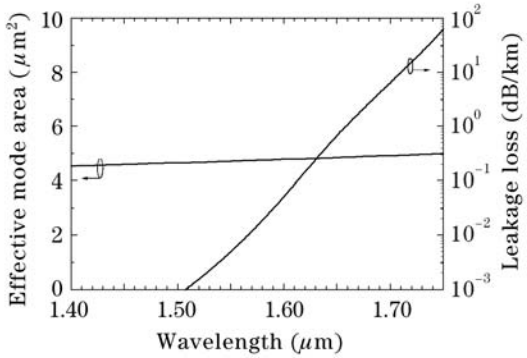

Fig. 5. Effective mode area and confinement loss as functions of wavelength for the optimized parameters, $\Lambda = 2.2$ μm, $\Lambda_y = 0.8\Lambda$, $d'/\Lambda = 0.85$, $d/\Lambda = 0.50$ and $N_r = 10$.

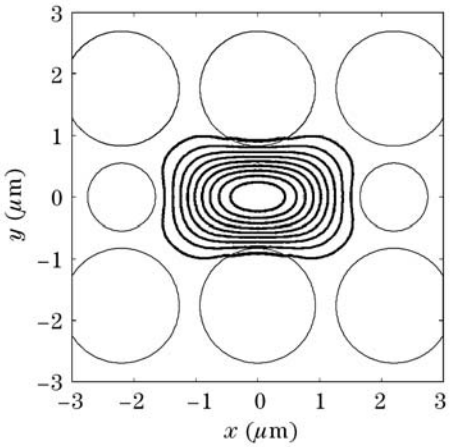

Fig. 6. Contour plot of intensity distribution of the x-polarized mode with $\Lambda = 2.2$ μm, $\Lambda_y = 0.8\Lambda$, $d'/\Lambda = 0.85$, $d/\Lambda = 0.50$ and $N_r = 10$ at $\lambda = 1550$ nm.

x-polarized mode in Fig. 6 at $\lambda = 1550$ nm, we can see that light is strongly confined to the core of the PCF. Notice that there is no higher order mode found within the wavelength region from 1370 to 1610 nm, so the proposed fiber functions as a SPSM fiber within this range, where only x-polarized mode exists and the confinement loss is less than 0.1 dB/km.

To summarize this paper, we have proposed a novel design for achieving SPSM operation at 1550 nm in PCFs by using a rectangular-lattice PCF with two lines of three central air holes enlarged. The fact that our proposed fiber structure possesses wide-band single-polarization operation mainly attributes to the degeneracy of the x- and y-polarized FSMs in the cladding region, which is realized by arranging the air holes in a rectangular lattice. In this paper, we only take $d/\Lambda = 0.5$ into consideration. In fact, for a larger or smaller value of d/Λ, PCF with similar cutoff properties can also be obtained by increasing or decreasing the value of the d'/Λ accordingly. Moreover, low confinement losses as well as small effective mode area characteristics are also shown in the proposed PCF. Other PCFs which can operate as SPSM fibers within the whole telecommunication window are currently under consideration.

This work was supported by the National Natural Science Foundation of China (No. 60507007), and the Program for New Century Excellent Talents in University (NCET, Min Zhang 2007). F. Zhang' e-mail address is frankmore21c@yahoo.com.cn.

References

1. J. C. Knight, T. A. Birks, P. St. J. Russell, and D. M. Atkin, Opt. Lett. **21,** 1547 (1996).
2. T. A. Birks, J. C. Knight, and P. St. J. Russell, Opt. Lett. **22,** 961 (1997).
3. R. F. Cregan, B. J. Mangan, J. C. Knight, T. A. Birks, P. St. J. Russell, P. J. Roberts, and D. C. Allan, Science **285,** 1537 (1999).
4. X. Zhang, X. Ren, Y. Xu, Y. Huang, and X. Chen, Chin. Opt. Lett. **5,** 11 (2007).
5. L. He, B. Yang, X. Zhang, and L. Yu, Chin. Opt. Lett. **4,** 715 (2006).
6. Z. Wang, X. Ren, X. Zhang, Y. Xu, and Y. Huang, Chin. Opt. Lett. **4,** 625 (2006).
7. H. Fang, S. Lou, G. Ren, T. Guo, and S. Jian, Chin. J. Lasers (in Chinese) **33,** 493 (2006).
8. J. Liu, C. Yang, C. Gu, and G. Jin, Acta Opt. Sin. (in Chinese) **26,** 1569 (2006).
9. A. Ortigosa-Blanch, J. C. Knight, W. J. Wadsworth, J. Arriaga, B. J. Mangan, T. A. Birks, and P. St. J. Russell, Opt. Lett. **25,** 1325 (2000).
10. K. Suzuki, H. Kubota, S. Kawanishi, M. Tanaka, and M. Fujita, Opt. Express **9,** 676 (2001).
11. M. Szpulak, J. Olszewski, T. Martynkien, W. Urbanczyk, and J. Wojcik, Opt. Commun. **239,** 91 (2004).
12. M. Chen, R. Yu, and A. Zhao, Opt. Commun. **241,** 365 (2004).
13. K. Saitoh and M. Koshiba, IEEE Photon. Technol. Lett. **14,** 1291 (2002).
14. J. R. Simpson, R. H. Stolen, F. M. Sears, W. Pleibel, J. B. Macchesney, and R. E. Howard, J. Lightwave Technol. **1,** 370 (1983).

15. K. S. Chiang, J. Lightwave Technol. **7,** 436 (1989).
16. M. J. Messerly, J. R. Onstott, and R. C. Mikkelson, J. Lightwave Technol. **9,** 817 (1991).
17. K. Saitoh and M. Koshiba, IEEE Photon. Technol. Lett. **15,** 1384 (2003).
18. H. Kubota, S. Kawanishi, S. Koyanagi, M. Tanaka, and S. Yamaguchi, IEEE Photon. Technol. Lett. **16,** 182 (2004).
19. J. Ju, W. Jin, and M. S. Demokan, J. Lightwave Technol. **24,** 825 (2006).
20. M. Koshiba and Y. Tsuji, J. Lightwave Technol. **18,** 737 (2000).
21. S. Lou, W. Jian, G. Ren, and S. Jian, J. Optoelectronics·Laser (in Chinese) **16,** 1265 (2005).
22. G. P. Agrawal, *Nonlinear Fiber Optics* (Academic Press, New York, 1995) p.7.
23. S. Li, G. Xing, G. Zhou, and L. Hong, Acta Phys. Sin. (in Chinese) **55,** 238 (2006).
24. T. P. White, R. C. McPhedran, C. M. de Sterks, L. C. Botten, and M. J. Steel, Opt. Lett. **26,** 1660 (2001).